The Origin of Hypervelocity Stars and GC S-stars, GC pulsars and hyperfast pulsars

Youjun Lu

National Astronomical Observatory of China

2016.02.08@Aspen

Collaborators: Fupeng ZHANG (SYSU)
Qingjuan YU (KIAA)

- **Constraining the spin of the massive black hole at the Galactic center via the motion of a surrounding star (Qingjuan YU)**

- **On testing the Kerr metric in the GC via star orbits: the effects of stellar perturbations (Fupeng ZHANG)**

Outline

- Background: GC S-stars, and hypervelocity stars
- Dynamical models: Tidal breakup of binary stars in the vicinity of the GC MBH
- Confronting observations with models
- Model predictions
- Summary

Introduction: evidence for an MBH in the GC

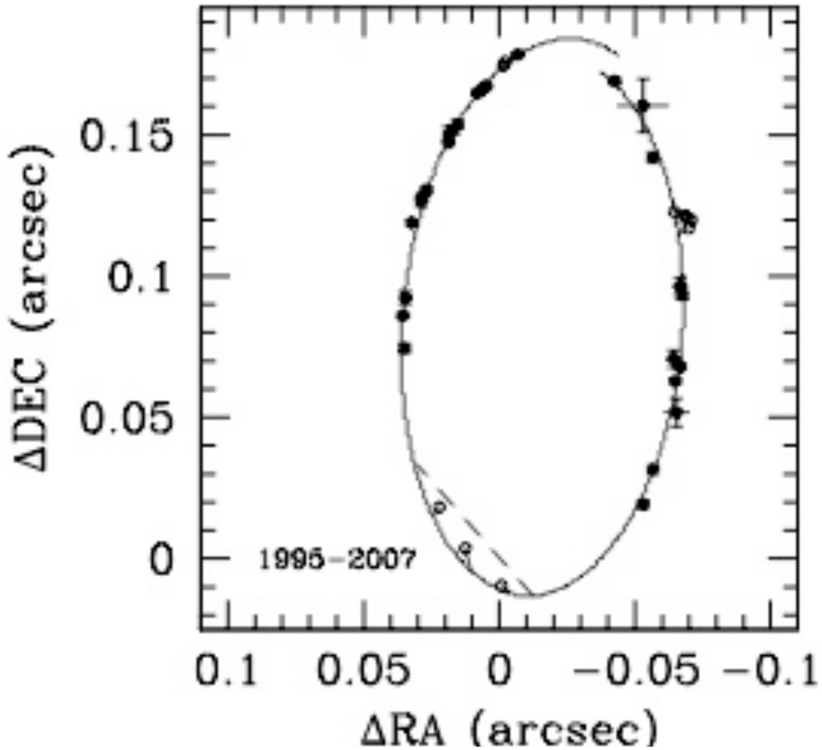

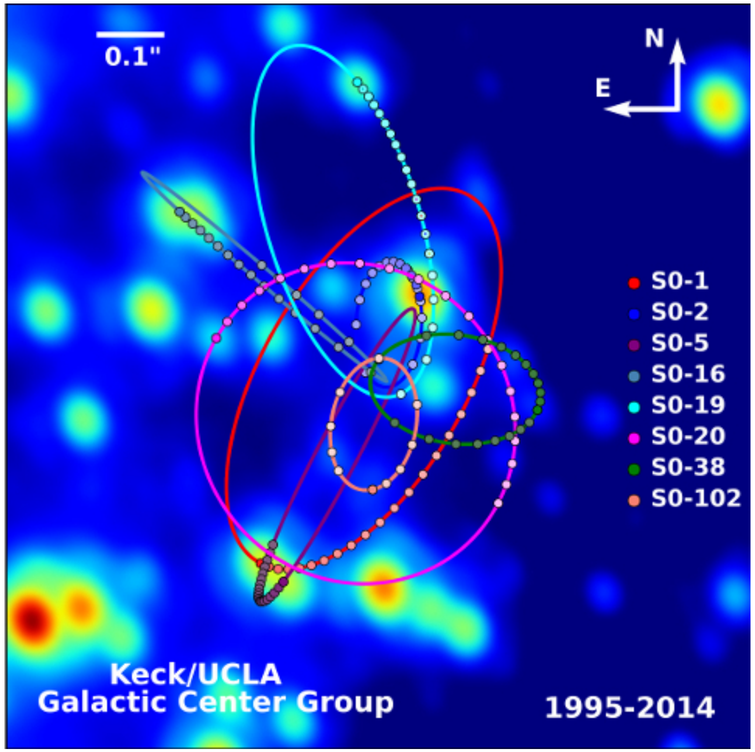

Velocities & Orbits of Stars → Mass

$$M_{\bullet} = rv^2 / G$$

$$M_{\bullet} = 4 \times 10^6 M_{\odot}$$

Ghez et al; Genzel, et al.

Introduction: Galactic center

A unique laboratory for stellar dynamics and black hole physics

❖ **Stellar structures in the Galactic Center (GC)**

- **Young stellar disk(s): 0.04-0.5pc**
  clockwise rotating stellar disk (CWS)
  + a counter clockwise disk?

- **S-stars: <4000AU (isotropic)**
  the closest one to the MBH (<1000AU)
  (S0-2/S2, S0-102)

Interplay between stars and MBH

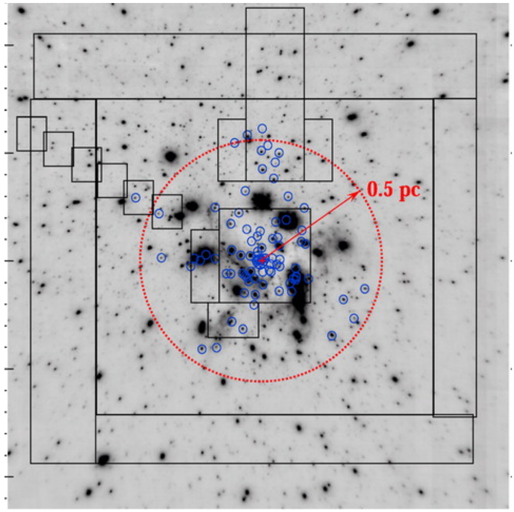

Introduction: formation of S-stars

- **Stellar disks:** stars were formed in a gaseous disk (in situ)
- **S-stars:** <4000AU (tidal force)
  - **Youth paradox:** (Ghez et al. 2003)
    - Rejuvenation of old stars?
    - Migration of stars from the stellar disk?
      (Madigan+ 2009; Baruteau+ 2011, Chen+ 2014)
    - **Exchange captures?** (Gould & Quillen 2003)
      Hills mechanism (tidal breakup of binaries)
- **What are the origins of the S-stars? Are there any bright stars closer to the central MBH than the known S-stars?**
- **Can the closest one be used to probe the metric of the GC MBH** or the distribution of background stars (stellar remnants)**?**

Alexander + Antonini + Chen + Perets + many other talks

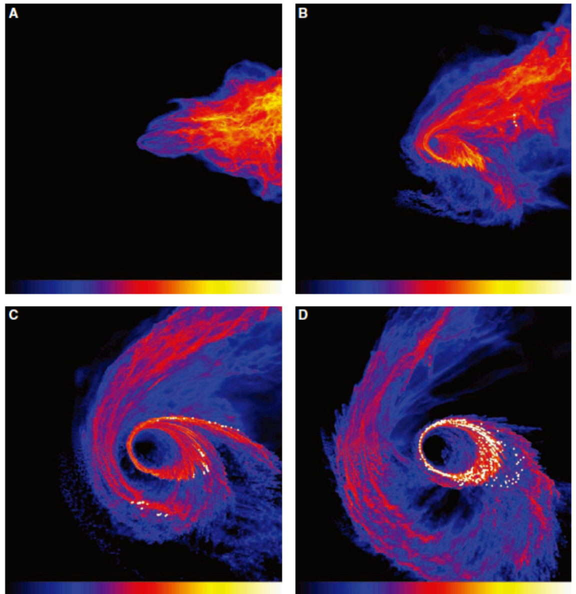

Fig. 1. The evolution of a $10^4\ M_\odot$ molecular cloud falling toward a $10^6\ M_\odot$ supermassive black hole. (**A**) The region within 1.5 pc of the black hole, ~32,000 years after start of evolution; colors denote the column density on a logarithmic scale from 0.01 g cm^{-2} to 100 g cm^{-2}. (**B**) Image at 42,000 years, showing the region within 1 pc of the black hole; color scale is from 0.025 g cm^{-2} to 250 g cm^{-2}. (**C** and **D**) Images at 47,000 and 51,000 years, showing the region within 0.5 pc of the black hole; color scale is from 0.1 g cm^{-2} to 1000 g cm^{-2}. Although the cloud is tidally disrupted by the black hole, some of the material is captured by the black hole to form an eccentric disk that quickly fragments to form stars. These are illustrated by the white dots and have eccentricities between e = 0.6 and e = 0.76 and semimajor axes between a = 0.11 pc and a = 0.19 pc. A small population of stars also forms quite early, becoming visible in (B) and being ejected from the system in (D).

Hypervelocity stars (HVSs) in the Galactic halo

Table 1
HVS Survey Stars with $v_{rf} > +275$ km s^{-1}

HVS	$v_{\odot}$ (km s^{-1})	v_{rf} (km s^{-1})	g_0 (mag)	T_{eff} (K)	log g (cm s^{-2})	$v \sin i$ (km s^{-1})	mass ($M_{\odot}$)	M_g (mag)	R_{GC} (kpc)	t_{flight} (Myr)	$(\mu_\alpha, \mu_\delta)_{GC}$ (mas yr^{-1})	Catalog
HVSs												
1	831.1 ± 5.7	673.1	19.688	11192 ± 450	3.91 ± 0.20	158 ± 36	3.23 ± 0.13	−0.36 ± 0.31	107 ± 15	138 ± 19	−0.09, −0.35	SDSS J090744.99+024506.89
4	600.9 ± 6.2	551.5	18.314	14547 ± 598	4.15 ± 0.21	77 ± 40	4.24 ± 0.16	−0.71 ± 0.33	70 ± 10	106 ± 16	−0.20, −0.77	SDSS J091301.01+305119.83
5	545.5 ± 4.3	650.1	17.557	12000 ± 350	3.89 ± 0.13	132 ± 37	3.58 ± 0.11	−0.67 ± 0.25	50 ± 5	66 ± 7	−0.45, −1.21	SDSS J091759.47+672238.35
6	609.4 ± 6.8	501.4	18.966	12190 ± 537	4.30 ± 0.23	170 ± 55	3.06 ± 0.11	+0.25 ± 0.27	58 ± 7	95 ± 12	−0.58, −0.66	SDSS J110557.45+093439.47
7	526.9 ± 3.0	402.0	17.637	12000 ± 500	3.80 ± 0.10	47 ± 35	3.76 ± 0.12	−0.95 ± 0.26	53 ± 6	103 ± 12	−0.65, −0.64	SDSS J113312.12+010824.87
8	499.3 ± 2.9	408.3	17.939	11000 ± 1000	3.75 ± 0.25	320 ± 60	3.42 ± 0.20	−0.69 ± 0.40	58 ± 10	112 ± 18	−0.32, −0.84	SDSS J094214.03+200322.07
9	616.8 ± 5.1	458.8	18.639	11637 ± 520	3.84 ± 0.21	306 ± 72	3.54 ± 0.16	−0.71 ± 0.34	77 ± 12	136 ± 21	−0.29, −0.45	SDSS J102137.08−005234.77
10	467.9 ± 5.6	416.7	19.220	11278 ± 524	4.38 ± 0.23	37 ± 60	2.65 ± 0.11	+0.65 ± 0.24	53 ± 6	100 ± 12	−0.73, −0.73	SDSS J120337.85+180250.35
12	552.2 ± 6.6	416.5	19.609	12098 ± 622	4.62 ± 0.28	78 ± 88	2.73 ± 0.14	+0.55 ± 0.28	67 ± 8	127 ± 17	−0.41, −0.55	SDSS J105009.59+031550.67
13	569.3 ± 6.1	423.9	20.018	11054 ± 775	4.00 ± 0.35	238 ± 43	3.05 ± 0.18	−0.10 ± 0.40	107 ± 19	201 ± 39	−0.22, −0.34	SDSS J105248.30−000133.94
14	537.3 ± 7.2	409.4	19.717	11030 ± 545	3.90 ± 0.24	162 ± 42	3.18 ± 0.15	−0.34 ± 0.35	105 ± 16	202 ± 32	−0.21, −0.38	SDSS J104401.75+061139.02
15	461.0 ± 6.3	328.3	19.153	11132 ± 526	4.05 ± 0.23	125 ± 44	2.99 ± 0.12	+0.05 ± 0.32	67 ± 10	149 ± 23	−0.46, −0.52	SDSS J113341.09−012114.25
16	429.8 ± 7.0	346.2	19.334	10388 ± 657	3.96 ± 0.29	259 ± 53	2.85 ± 0.15	+0.08 ± 0.35	71 ± 12	152 ± 26	−0.50, −0.51	SDSS J122523.40+052233.84
17	250.2 ± 2.9	435.8	17.427	12350 ± 290	3.80 ± 0.09	96 ± 42	3.91 ± 0.09	−1.06 ± 0.19	49 ± 4	89 ± 8	−0.69, +0.00	SDSS J164156.39+472346.12
18	237.3 ± 6.4	446.2	19.302	11993 ± 507	4.08 ± 0.21	96 ± 41	3.27 ± 0.12	−0.14 ± 0.30	80 ± 11	143 ± 21	+0.39, −0.16	SDSS J232904.94+330011.47
19	592.8 ± 11.8	492.0	20.061	12900 ± 784	4.53 ± 0.29	137 ± 78	3.12 ± 0.17	+0.12 ± 0.34	98 ± 15	164 ± 28	−0.31, −0.39	SDSS J113517.75+080201.49
20	512.1 ± 8.5	396.6	19.807	11149 ± 640	4.21 ± 0.28	275 ± 46	2.79 ± 0.12	+0.42 ± 0.31	76 ± 11	150 ± 24	−0.41, −0.48	SDSS J113637.13+033106.84
21	356.8 ± 7.5	391.9	19.730	13229 ± 950	4.16 ± 0.31	65 ± 88	3.70 ± 0.21	−0.44 ± 0.42	113 ± 21	224 ± 47	−0.18, −0.45	SDSS J103418.25+481134.57
22	597.8 ± 13.4	488.7	20.181	11145 ± 850	4.35 ± 0.30	94 ± 68	2.66 ± 0.16	+0.56 ± 0.34	85 ± 13	142 ± 25	−0.38, −0.43	SDSS J114146.44+044217.29
23	259.3 ± 9.8	423.2	20.201	10996 ± 768	3.99 ± 0.29	48 ± 88	3.04 ± 0.16	−0.10 ± 0.38	112 ± 20	210 ± 40	+0.12, −0.30	SDSS J215629.01+005444.18
24	492.5 ± 5.3	357.6	18.855	11231 ± 542	4.12 ± 0.24	179 ± 43	2.93 ± 0.12	+0.19 ± 0.30	56 ± 7	117 ± 17	−0.55, −0.63	SDSS J111136.44+005856.44

- **Escaping away from the Milky way halo (hypervelocity)**
- **Distance from ~40kpc to ~120kpc from the GC**
- **Mainly type B stars (3-4$M_{\odot}$)**

Brown et al. 2014, 2015

Hypervelocity stars (HVSs)

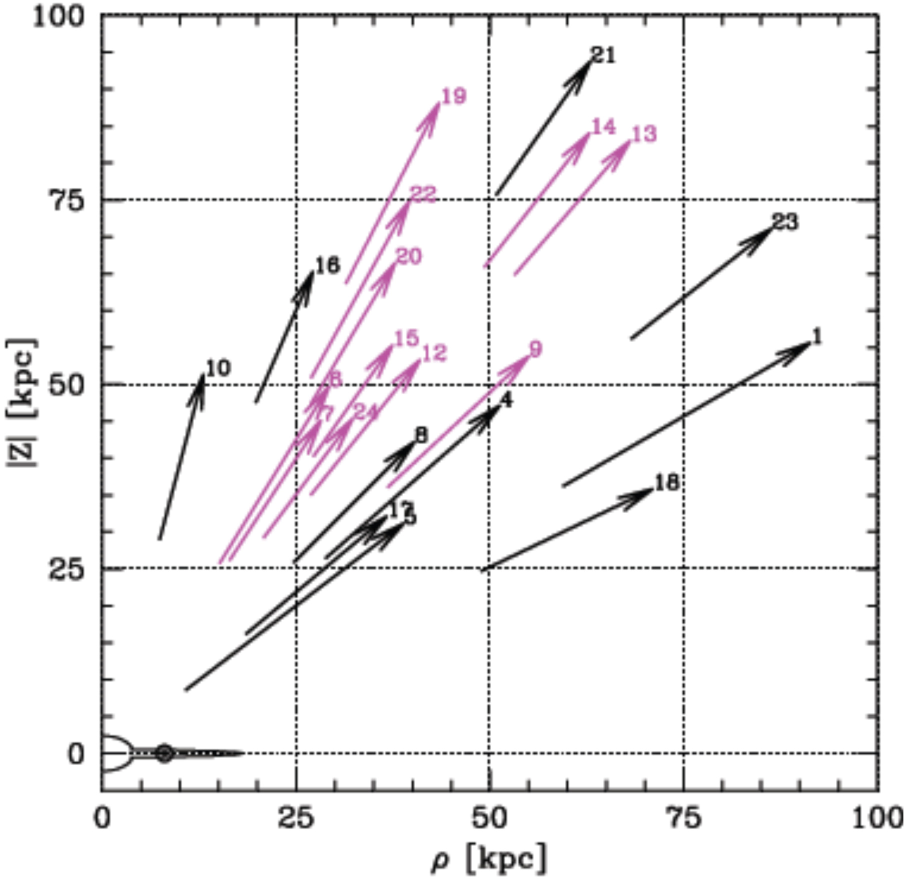

Figure 5. HVSs plotted in Galactic cylindrical coordinates. Arrow lengths are scaled to v_{rf}, and arrow tips are located at the present positions of the HVSs. Magenta arrows are those objects clumped together around Leo.

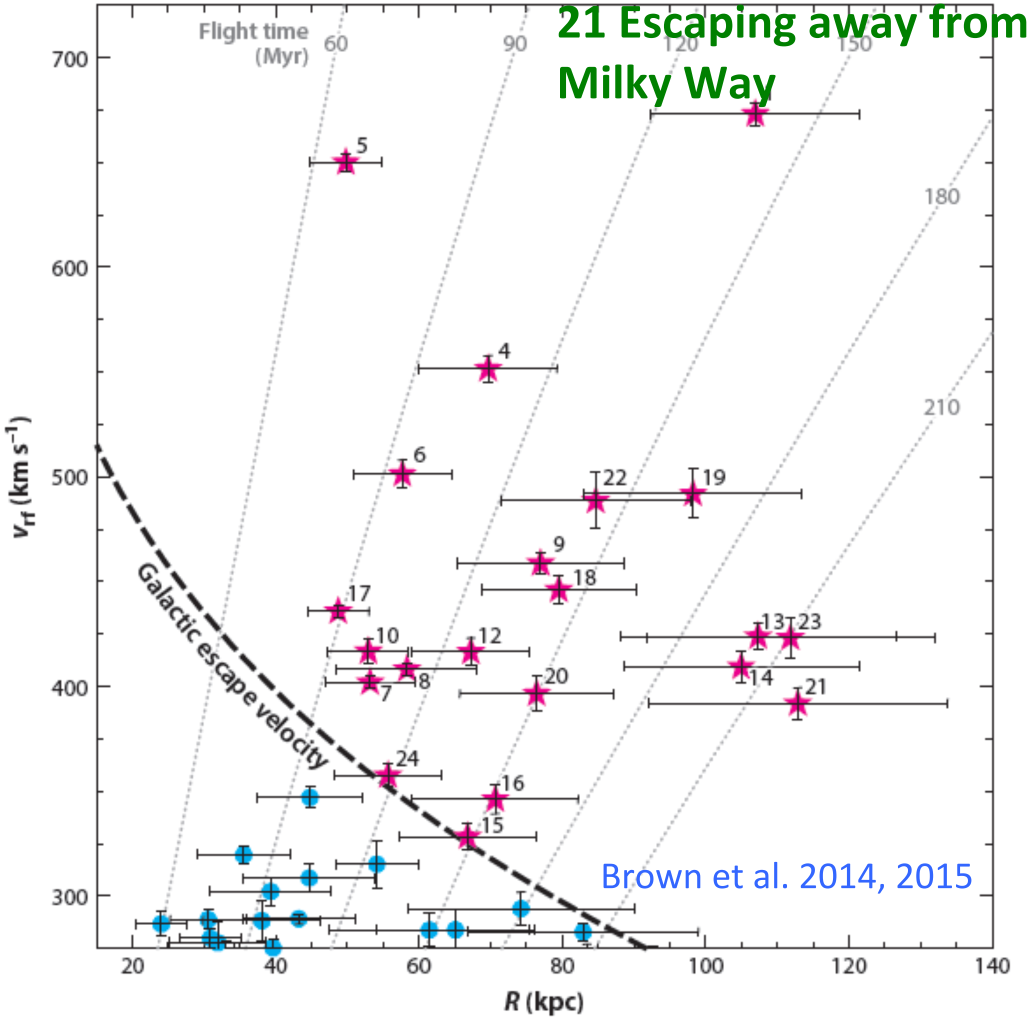

21 Escaping away from Milky Way

HVSs as a prediction of Hills mechanism (and others) are detected by later observations!

Tidal breakup of binary stars

(Hills 1988; Yu & Tremaine 2003)

❖ **Tidal breakup of binary stars in the vicinity of the MBH**

- **captured component: S-star (<4000AU)** (Gould & Quillen 2003)
- **ejected component: hypervelocity star (>700km/s)**

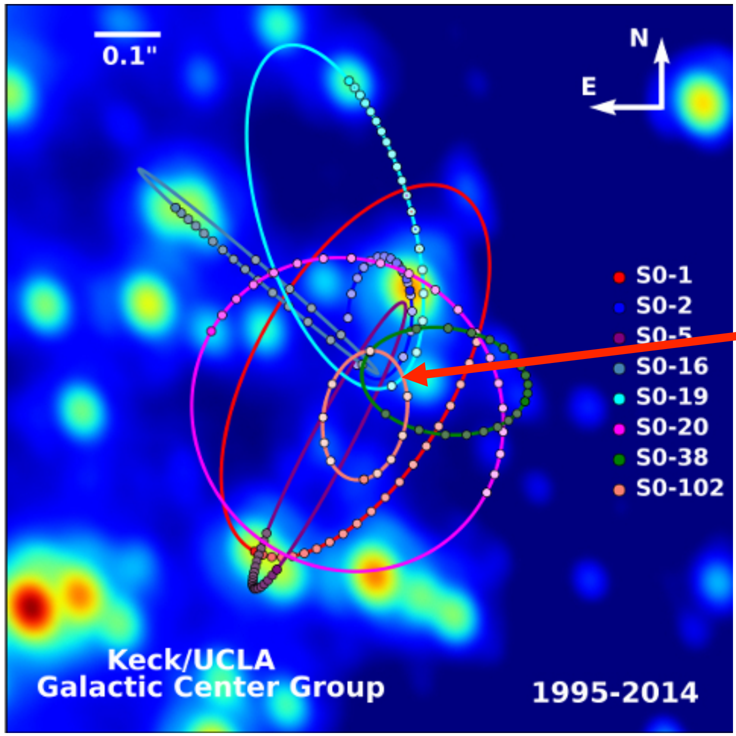

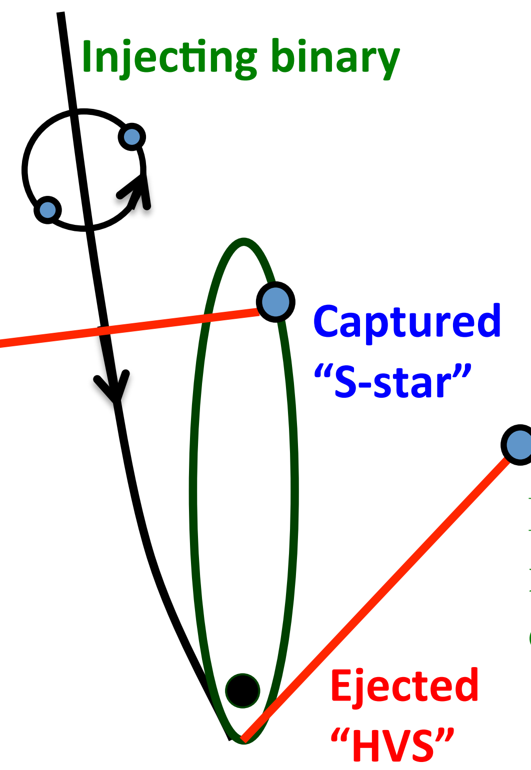

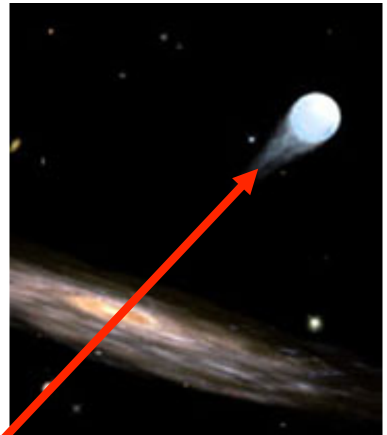

HVSs as a prediction of the Hills mechanism (and others) are confirmed by later observations!

Tidal breakup of binary stars

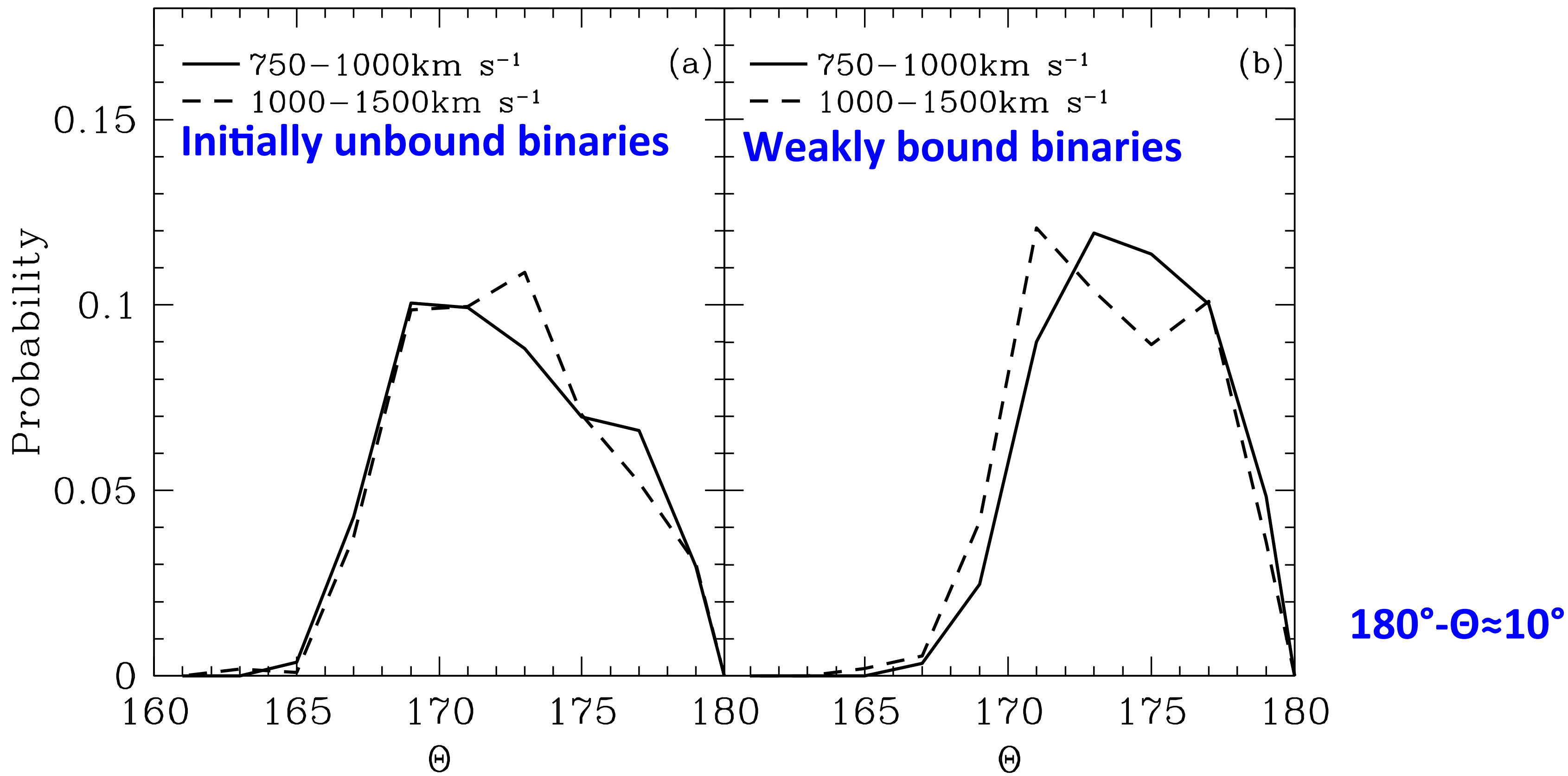

HVSs can well memorize the injecting directions of their progenitors, i.e., the ejecting direction of an HVS is almost anti-parallel to the injecting direction of its progenitor.

Lu et al. 2010
Zhang et al. 2010

Summary on the observational statistics for HVSs and GC S-stars

HVSs:

- **Mass**
  ~3-4$M_\odot$; B-type
- **Number: ~21(24) (~100)**
- **Spatial distribution: anisotropic**
- **Distance distribution**
- **Velocity distribution**

Consistent? ⟷

S-Stars

- **Mass**
  ~7-15$M_\odot$; B-type
- **Number: ~17 (<4000AU)**
- **Spatial distribution: isotropic**
- **Semi-major axis distribution**
- **Eccentricity distribution**

Dynamics of HVSs and S-stars:
assuming Hills mechanism

Model ingredient	HVSs	S-Stars
Injecting stellar binaries	From the stellar disk or from infinity; (slowly) scatter to the loss cone; 1-150$M_\odot$; semimajor axis and mass ratio distributions of the binaries; IMF: intermediate top-heavy or others	
Tidal breakup	Ejected	Captured (full 3-body)
Later dynamical evolution	Transport from the GC to the Galactic halo	✧ Non- and Resonant relaxations; ✧ GR precession and Gravitational wave decay.
Stellar evolution	Main sequence or pulsar, SN kick	

Lu (with Zhang and Yu: 2010a; 2010b; 2013; 2014)

ARMA model by Madigan et al.

Confronting observations with models: velocity distribution of HVSs

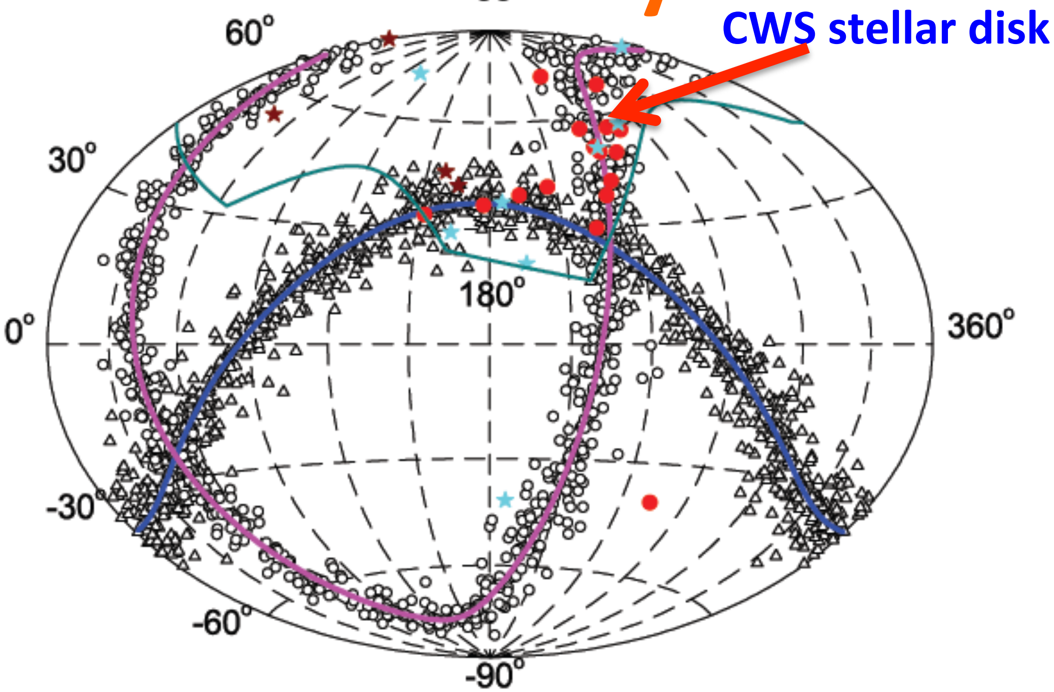

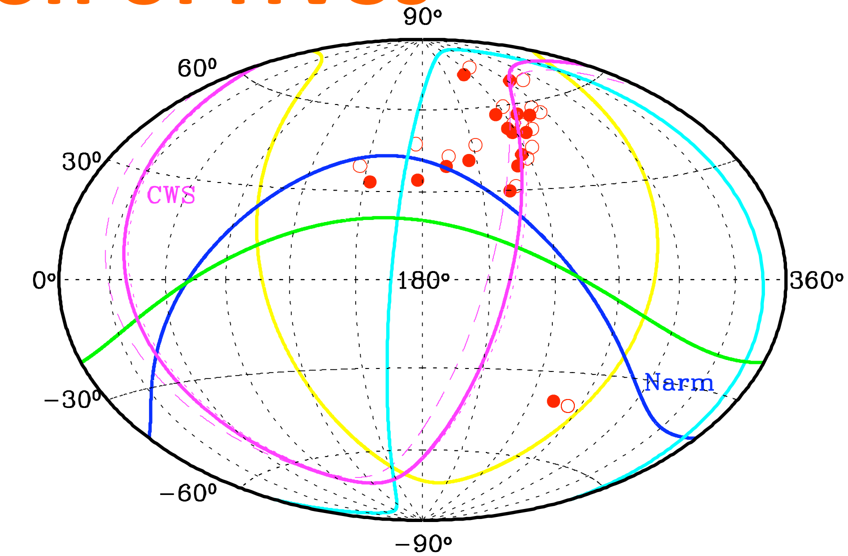

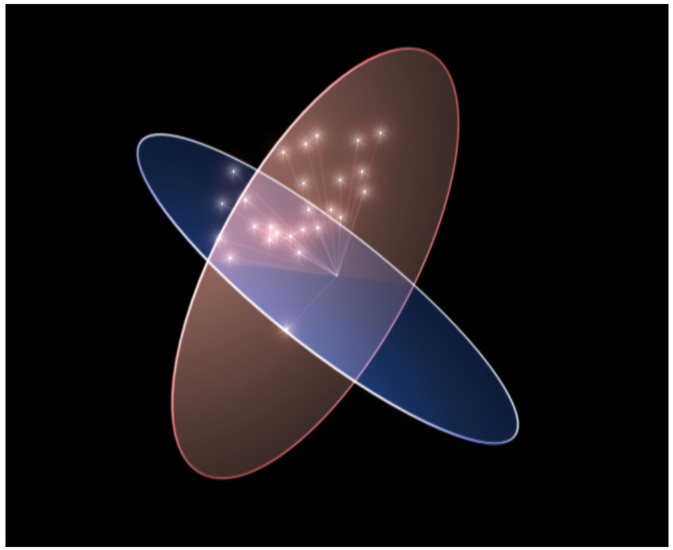

- **Reproducing most HVS statistics:**
  - theory: memory of injecting direction;
  - observation: consistent with being on two disk planes, one of which is the same as that of the CWS disk in the GC;
  - conclusion: HVS probably originated from the GC disk(s).

Lu et al. 2010

HVSs from LAMOST

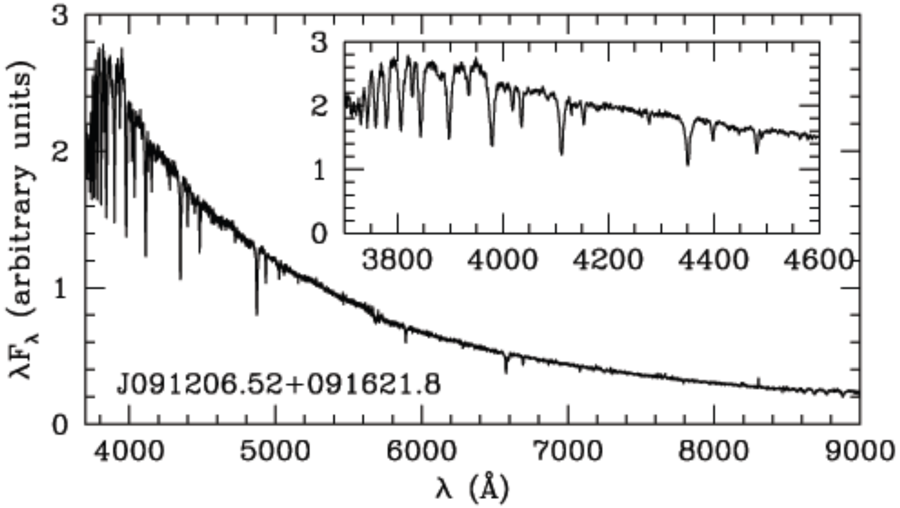

Figure 1. Spectrum of LAMOST-HVS1 taken with the Guo Shoujing Telescope. The inset shows a close-up view of the blue end of the spectrum.

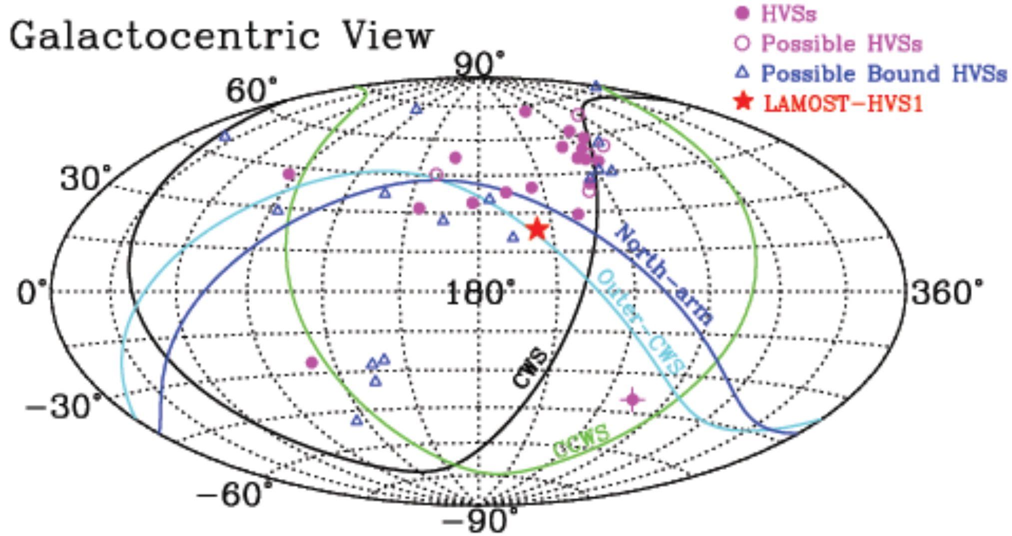

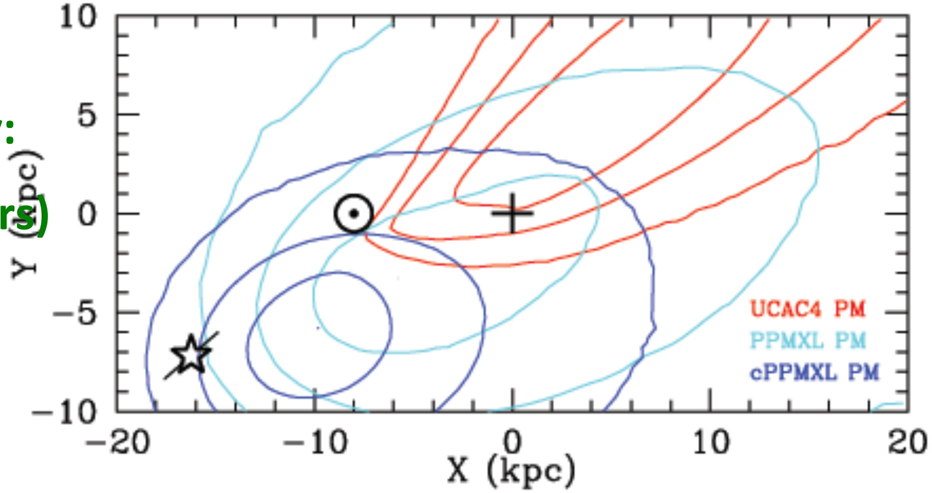

An HVS found in the LAMOST Galactic survey:

- Mass: ~9$M_\odot$ (possible companion of S-stars)
- Velocity: v_{rf}=477km/s (~545km/s)
- Location: ~19kpc (Galactocentric dist.)
- GC origin: consistent

Another one is recently found in LAMOST.

Zheng et al. 2014

Confronting observations with models:
velocity distribution of HVSs

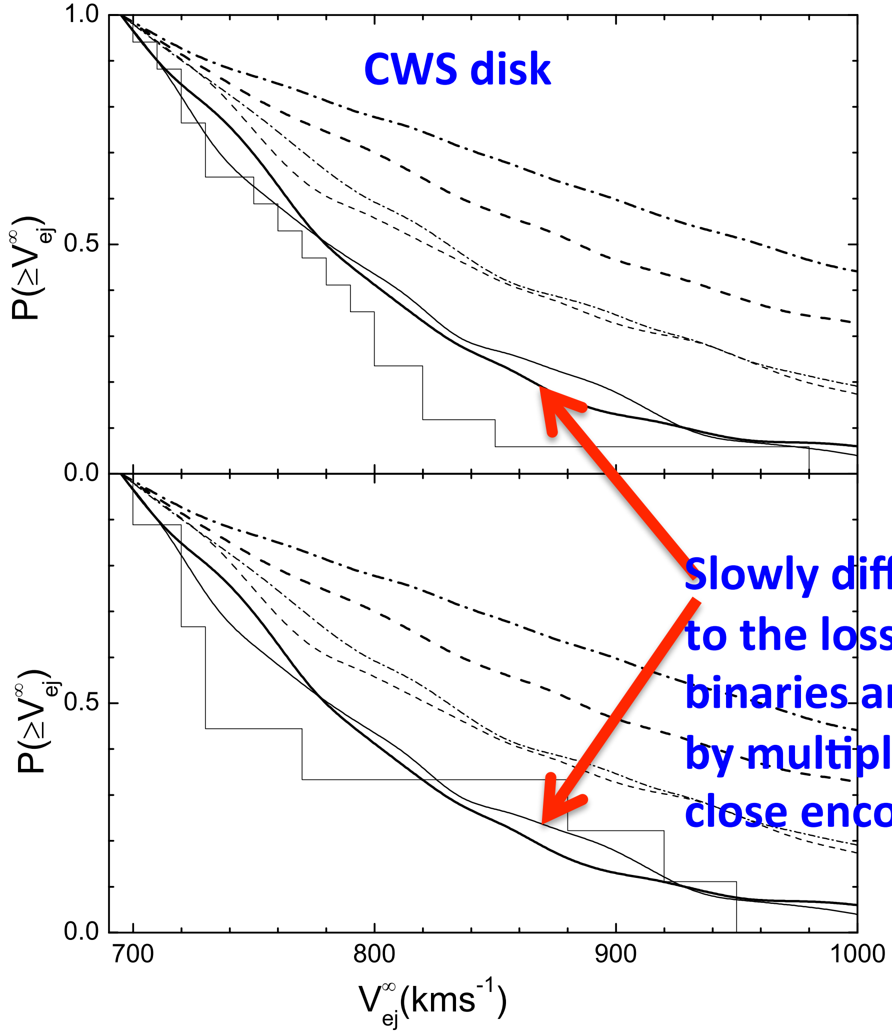

Slowly diffused to the loss cone, binaries are disrupted by multiple times of close encounter .

Assuming several Galactic potential

Main factors:

- **The initial distribution of the semimajor axes of injecting binaries;**
- **The perturbation that causes the injection of binaries.**

Can be well reproduced if binary stars perturbed onto low-J orbits by diffusion processes/random walk or ΔJ<<J.

Large perturbations lead to too flat velocity distribution.

Elena Rossi and Reem Sari's talks

Empty loss cone: slowly diffused

Through the boundary of the loss cone

Zhang et al. 2010

Confronting observations with models: S-stars

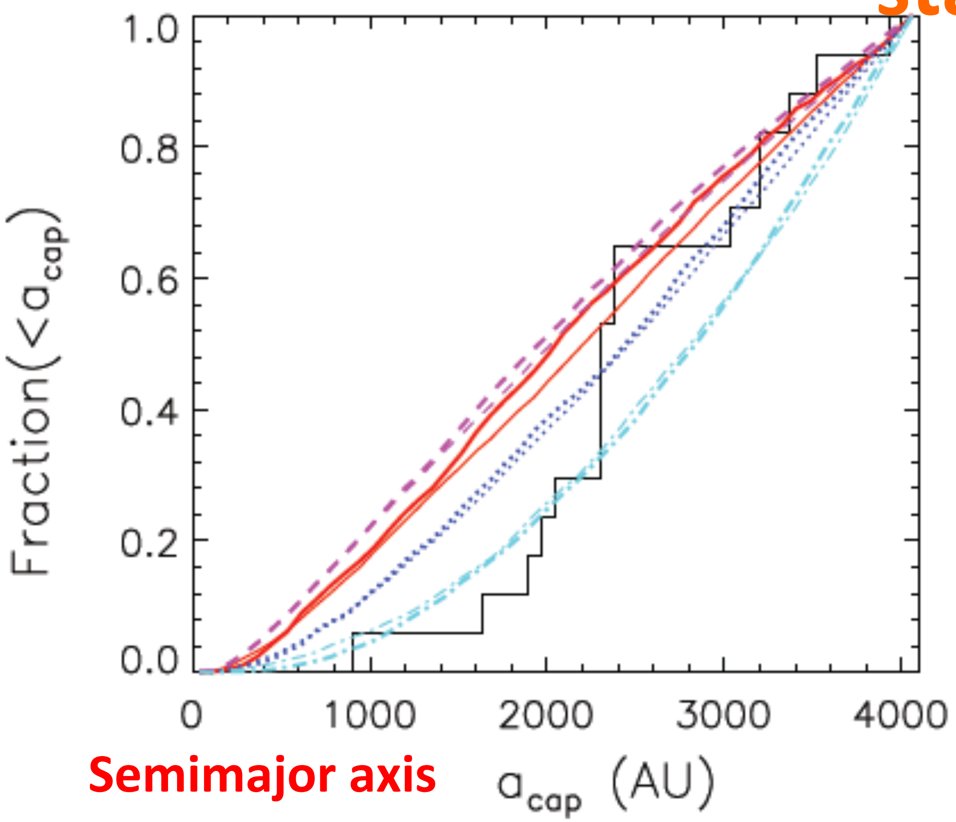

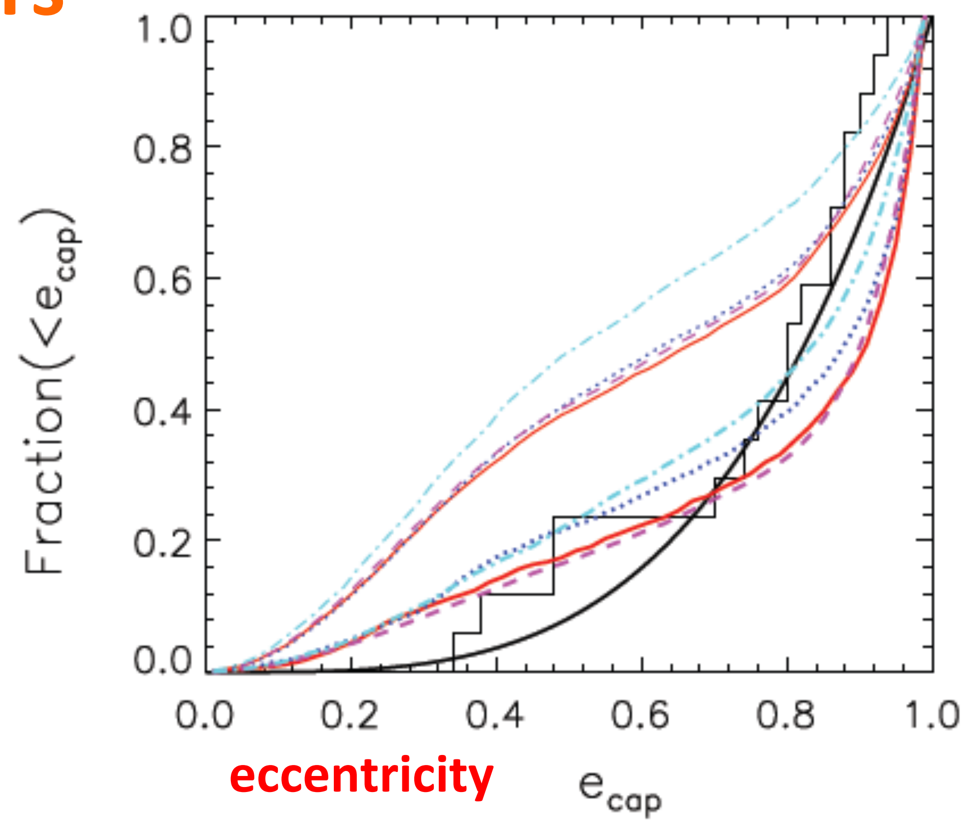

- **Reproducing most of the S-star statistics**
  - **semi-major axis distribution**
    (importance of relaxation resonance and GR dynamics)
  - **eccentricity distribution**

Lu with Zhang & Yu (2010; 2013)

Stellar mass function: top heavy

- **The number ratio of HVSs/S-stars can be re-produced if the stellar initial mass function is top-heavy, with MF slope ~−1.6 (**a requirement**).** Zhang, Lu, & Yu 2013
  - **A steeper IMF leads to a too large number ratio of HVSs to GC S-stars; a shallower one-> a too small nubmer ratio.**

- **Recent observation suggests that the IMF slope of the young cluster in the GC is -1.7±0.2, consistent with our model result.**

A further support for the common origin of the GC S-stars and the HVSs.

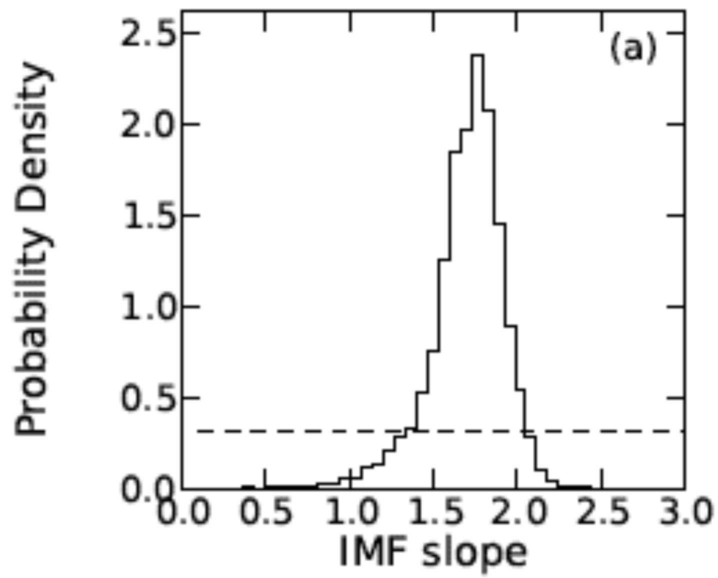

(Lu, J. et al., 2013; Jessica's talk)

Model predictions

- **Locations of HVSs at the southern heimsphere**
- **Ejected companions of the S-stars:**
  - ~20 - 60 detectable HVSs (~7-15$M_{\odot}$) in the Galactic bulge and halo
  - located in a distance <30kpc from the GC, radial velocity ～−500-1500 km/s, and proper motion ~5-20mas/yr (the first HVS found by LAMOST ~9$M_{\odot}$)
- **Captured companions of the detected HVSs**
  - ~20-30 captured stars (~3-7$M_{\odot}$) in the GC (≲4000AU)
  - the innermost one: ~300-1000AU
- **Pulsars in the GC**
  - ~100 within 4000AU; ~10 within 1000AU (also Pfahl & Loeb2004, Dexter &O'Leary 2014)
  - the innermost one: ~120-460AU
- **Hyperfast pulsars in the Galactic halo** (resulting from explosion of massive HVSs and S-stars)
  - ~several to ten hyperfast pulsars (>1500km/s)

Model predictions: the innermost captured star with mass ~3-7$M_\odot$

Testing GR

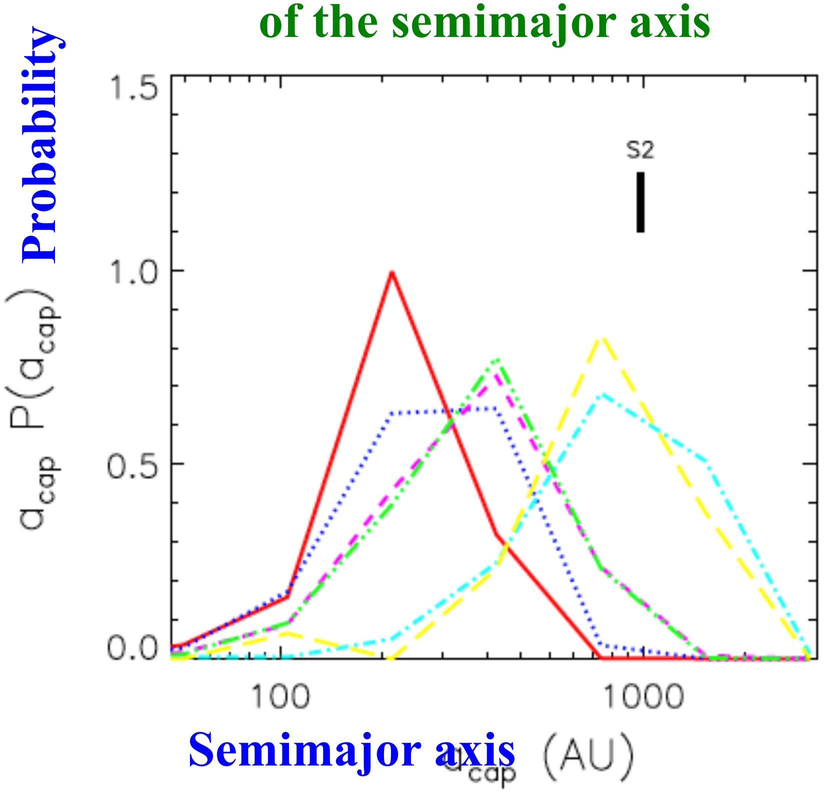

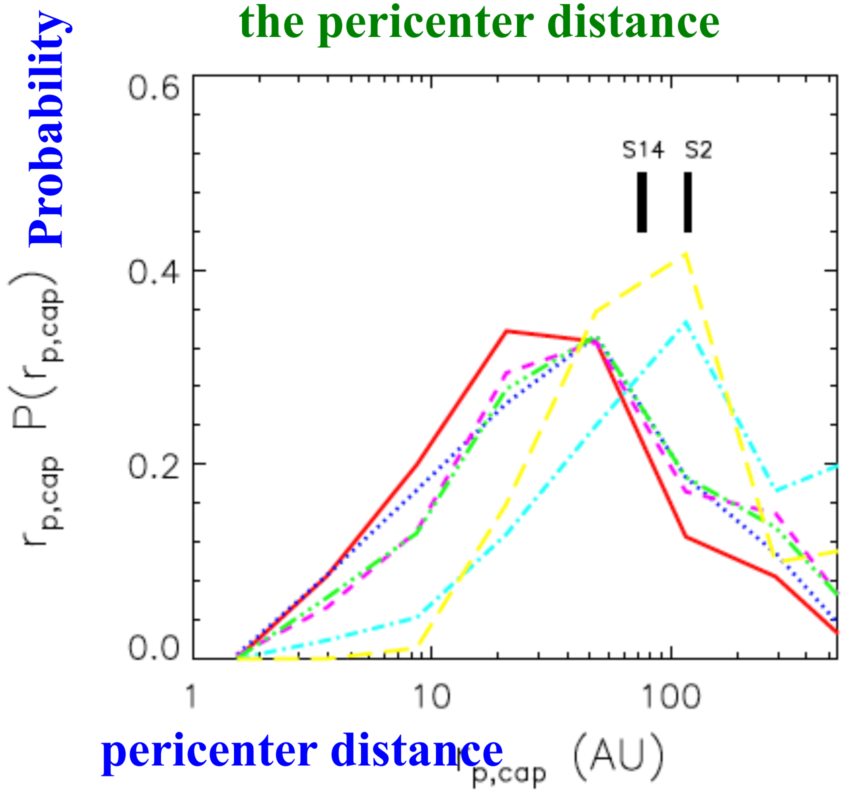

The innermost one is expected to have a semimajor axis ~300–1500AU and a pericenter distance ~10–200AU (depending on different injection models) with a significant probability of being closer to the MBH than S2.

(Zhang, Lu, & Yu, 2013, 2014)

Model predictions: the closest star to the MBH

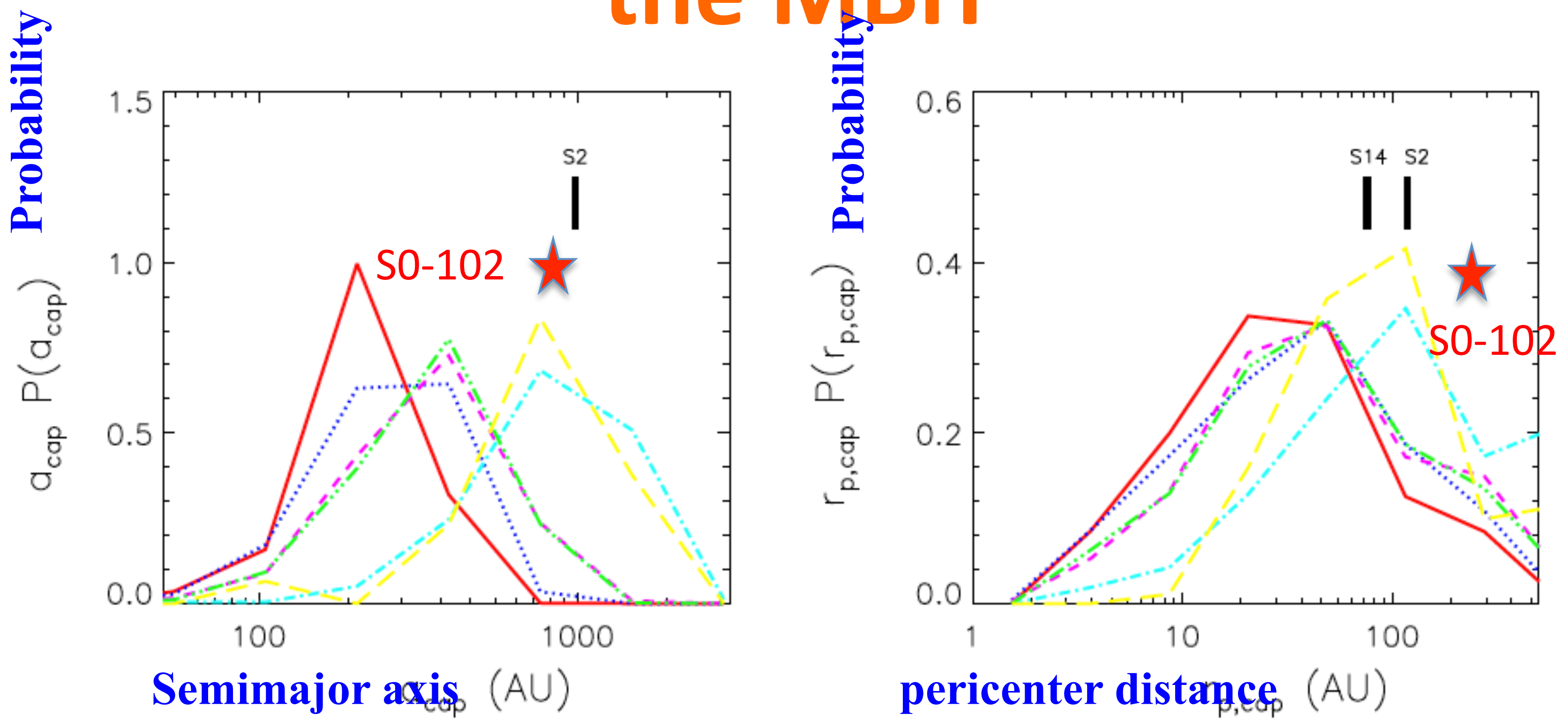

The predicted probability distribution of the semimajor axis and pericenter distance of the closest star is well consistent with the new observations.

Zhang et al. (2013, 2014)

Model predictions: the closest pulsar to the MBH

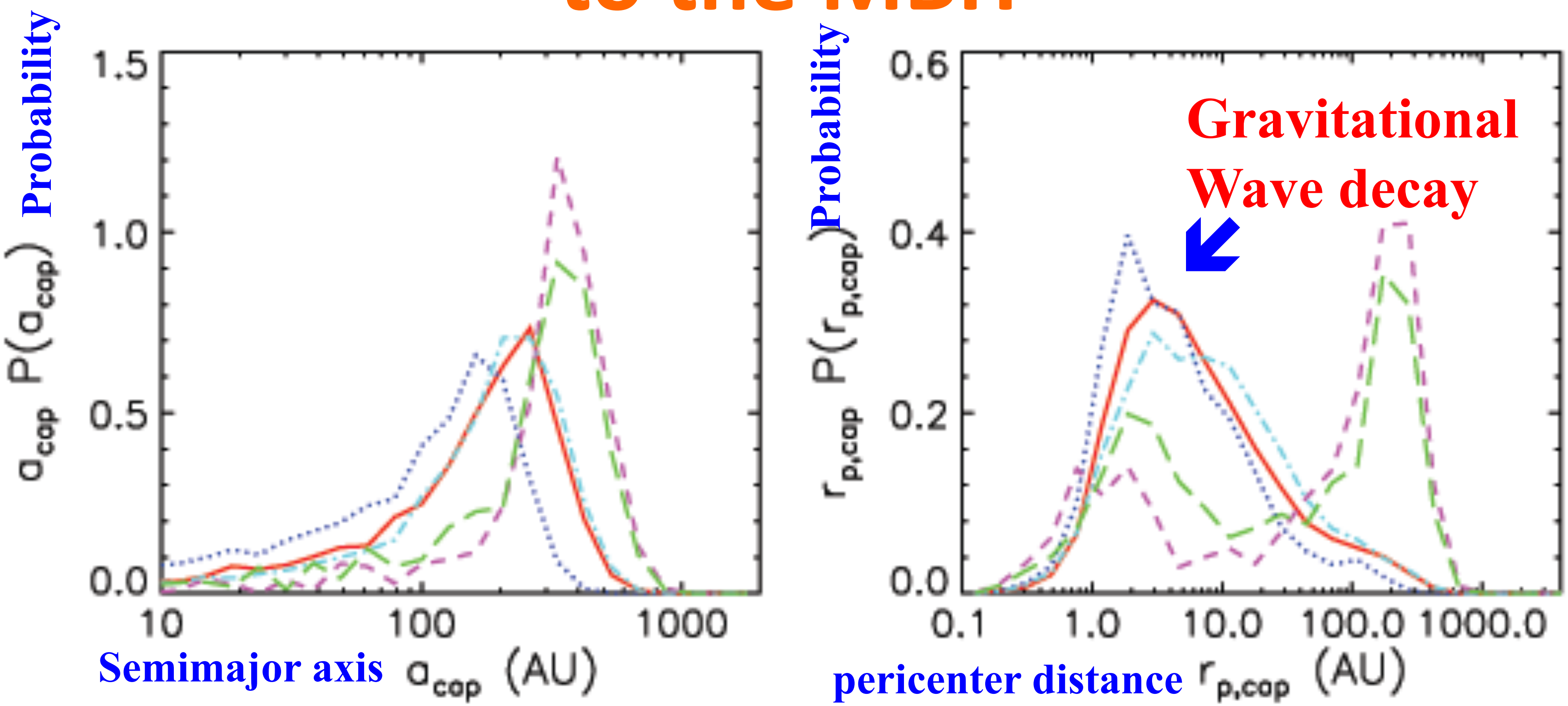

The predicted probability distribution of the semimajor axis and pericenter distance of the closest pulsar to the central MBH.

(even closer to the MBH than the captured S-stars)

Zhang, Lu, & Yu (2014)

Summary

- **Almost all the discovered HVSs are spatially consistent with being located on two thin disk planes, similar to the orientations of some GC structures (CWS disk and North arm of the mini-spiral?), which supports the GC origin.**
- **We investigate the link between the HVSs and the GC S-stars under the hypothesis that they both are the products of tidal breakup of the same population of stellar binaries by the central MBH. Most of the statistical properties of the detected HVSs and GC S-stars could be reproduced under some binary injecting models.**
- **We predict the statistical distributions of their companions (ejected companions for GC S-stars and captured companion for HVSs) and the pulsars resulting from those ejecting stars and captured stars, which may be tested by future observations.**